JBUON 2020; 25(3): 1413-1422
ISSN: 1107-0625, online ISSN: 2241-6293 • www.jbuon.com
Email: editorial_office@jbuon.com

ORIGINAL ARTICLE

# Dendritic cell-derived exosome-entrapped fluorouracil can enhance its anti-colon cancer effect

Man Xu[1]*, Qian Chen[2]*, Juan Li[1], Li Peng[2], Ling Ding[3]

[1]Department of Lymphoma, Cancer Center, Union Hospital, Tongji Medical College, Huazhong University of Science and Technology, Wuhan 430022, China. [2]Department of Bone and Soft Tissue Oncology, Cancer Center, Union Hospital, Tongji Medical College, Huazhong University of Science and Technology, Wuhan 430022, China. [3]Department of Gynecologic Oncology, Hubei cancer Hospital, Tongji Medical College, Huazhong University of Science and Technology, Wuhan 430079, China.

*These authors contributed equally to this work.

## Summary

***Purpose:*** *To explore the effectiveness of fluorouracil (FU) entrapped in dendritic cell (DC)-secreted exosomes (DC-Exos) for enhancing its anti-colon cancer effect.*

***Methods:*** *DC-Exos were extracted through ultrahigh-speed centrifugation, and the FU-DC-Exos system was constructed using electroporation. Moreover, the influence of FU-DC-Exos on the viability of mouse colon cancer CT26 cells was determined in vitro using 3-(4,5-dimethylthiazol-2-yl)-2,5-diphenyl tetrazolium bromide (MTT) assay and 4',6-diamidino-2-phenylindole (DAPI) staining, and pharmacodynamic evaluation was performed in vivo through TUNEL and hematoxylin-eosin (H&E) staining, with the CT26 tumor-bearing mouse model as the study object.*

***Results:*** *Compared with the control group, FU and DC-Exos groups exhibited a lowered proliferation rate of mouse CT26 colon cancer cells, whereas the apoptosis rate of cells in FU-DC-Exos group differed significantly from FU group. According to the wound healing assay, the migration rate of CT26 cells was reduced in FU and DC-Exos groups, and it was evidently different between FU-DC-Exos group and FU group. Moreover, in vivo experiments revealed that DC-Exos alone exhibited a trend of suppressing tumor growth, and that DC-Exos as carriers not only killed tumor cells alone, but also enhanced the anti-colon cancer effect of FU after entrapment.*

***Conclusions:*** *Exos extracted via ultrahigh-speed centrifugation can be used for the preparation of the drug delivery system of FU-DC-Exos via electroporation, and drug-loaded Exos are able to effectively inhibit the proliferation of tumor cells and induce their apoptosis, exerting an anti-tumor effect.*

***Key words:*** *DC-Exos, FU-DC-Exos, CT26 cells, apoptosis*

## Introduction

Tumors are the most destructive diseases and cause several million deaths each year. As published by the World Health Organization in 2012, 13% of the total deaths are attributed to tumors [1]. The morbidity rate of colon cancer is increasingly higher in recent years, as the diet and living habits of humans change. Conventional surgical treatment, radiotherapy and chemotherapy are still the main treatments for malignancies. The current sale of anti-cancer drugs accounts for a large proportion in the global medical market. Fluorouracil (FU) has a wide anti-tumor spectrum, and it is efficacious to a certain degree for colon cancer, gastrointestinal cancer, breast cancer and bladder cancer. However, FU is characterized by low lipid solubility, irregular oral absorption and low bioavailability, so it is generally intravenously administered. Persistent infusion can maintain an effective plasma concen-

*Corresponding author:* Ling Ding, MM. Department of Gynecologic Oncology, Hubei Cancer Hospital, Tongji Medical College, Huazhong University of Science and Technology, Wuhan 430079, China.
Tel: +86 013476003774, Email: 395639940@qq.com
Received: 19/12/2019; Accepted: 28/12/2019

tration in the body in a relatively long time, and has a better clinical efficacy than intravenous injection, but infusion for a long time decreases the compliance of patients. Additionally, FU produces a high incidence rate of intense toxic side effects, such as severe myelosuppression and gastrointestinal toxicity. All these shortcomings greatly limit the clinical application of FU [2].

In recent years, nanoscale drug carriers have gradually become the hotspots of research on tumors, and they can deliver hydrophobic drugs and possess unique pharmacokinetics. For example, liposomes [3], micelles [4], vesicles [5] and gold nanoparticles [6] have been researched deeply. Ideal carriers should be safe and efficacious, with optimal bioavailability. Meanwhile, the stability and low cytotoxicity and immunogenicity of carriers, whether drugs are successfully delivered into the specific tissues or cells, and carriers' own anti-tumor activity are vital as well [7,8]. Exosomes (Exos) derived from organisms themselves or cells have gradually attracted the attention of researchers. As drug delivery system, Exos have a series of advantages: (1) The drug-loaded Exos collected from the tissues or blood of patients (such as bone marrow, monocytes or macrophages) can escape the scavenge by the mononuclear phagocyte system, thereby lowering the clearance rate of drugs [9]. (2) With the potential targeting effect, Exos can enhance the ability to deliver the drugs to the target tissues [10]. (3) More importantly, the specific liposomes and proteins on the membranes of Exos enable Exos to directly fuse with the target cell membranes, thus significantly raising the chance of drugs entering cells [11]. (4) The carriers of Exos can evade the internalization by the endocytic pathway, and the safety of Exos has been corroborated by many clinical trials [12-15]. (5) Exos specifically carry ribonucleic acids (RNAs), proteins and other components from parent cells in secretion, and share the characteristics with parent cells. Therefore, more and more researchers have started to pay attention to the possibility of Exos as carriers and the value of their clinical application.

Exos are a class of cell-secreted nano-sized membrane vesicles with a diameter of 30-150 nm and mainly composed of lipid bilayers and proteins. They are extensively present in the body fluids and can be secreted by multiple cells such as erythrocytes, antigen-presenting cells, T cells, tumor cells and platelets. The most important is that Exos will specifically carry the components of parent cells in secretion, such as RNAs and proteins, to the specific sites through humoral transport, thereby participating in signal transduction *in vivo*, tumor immune evasion and treatment of related diseases [16,17]. Hence, the contents carried by Exos vary due to the origin and physiological status of parent cells, and the functions of Exos are closely related to parent cells. According to literature reports, dendritic cell-secreted Exos (DC-Exos) not only directly kill melanoma cells through the TNF superfamily ligands, but also induce tumor regression in the mouse model of orthotopic liver cancer [18,19]. Therefore, FU was entrapped in DC-Exos as the carrier of FU by the electroporation method in this study, and it was found that the preparation FU-DC-Exos containing the same dose of FU obviously inhibits the proliferation of colon cancer cells, showing preferable efficacy.

## Methods

*Reagents and animals*

Mouse colon cancer CT26 cells were purchased from Shanghai Cell Bank, Chinese Academy of Sciences; fetal bovine serum (FBS), Roswell Park Memorial Institute 1640 (RPMI 1640) medium and double antibodies from Gibco, Rockville, MD, USA; cluster of differentiation (CD) 9, Alg2-interacting protein X (Alix) and tumor-susceptibility gene 101 (TSG101) antibodies from Abcam, Cambridge, MA, USA; FU from Sigma, St. Louis, MO, USA; Tecnai G2 Spirit BioTwin biological transmission electron microscope (TEM) from USA; L-90K ultracentrifuge from Backman, USA; and nanoparticle tracking analysis (NTA) system from Malvern Panalytical. A total of 50 specific pathogen-free BALB/c mice aged 5 weeks old were provided by Huazhong University of Science and Technology, and the experiment was approved by the Animal Ethics Committee of Huazhong University of Science and Technology.

*Cell culture*

Mouse marrow DCs were isolated and cultured as follows: After the BALB/c mice were killed via cervical dislocation, the femur and tibia were aseptically separated, and the tissues were cleared with sterile gauze. Then bone marrows were pumped into a centrifuge tube, added with erythrocyte lysis buffer, and let stand for 5 min. Subsequently, RPMI 1640 was added to terminate the lysis, and the resulting products were centrifuged twice, followed by cell counting and sub-cultured using a conventional complete medium containing 20 ng/mL IL-4, 20 ng/mL GM-CSF, 10% FBS and 1% double antibodies.

Exo-free FBS was prepared according to the following steps [20]: FBS was centrifuged at 120,000 g for 16 h, and with 5% of the precipitates at the tube bottom discarded, the Exo-free FBS was harvested, sterilized using a 0.45 μm filter and stored at -80°C for later use.

*Extraction of Exos*

Exos were extracted and isolated via ultrahigh-speed differential centrifugation [21]: The culture supernatant of cells was collected and centrifuged succes-

sively at 300 g (10 min), 2,000 g (10 min), and 1,000 g (30 min) to remove cells and cell debris. After filtering using a 0.22 μm filter membrane, the filtrate was centrifuged at 120,000 g for 2 h, and the supernatant was removed. The precipitates were re-suspended using an appropriate amount of Exo-free phosphate buffered saline (PBS) and centrifuged again at 120,000 g for 2 h to eliminate possibly residual proteins. Subsequently, the concentration of Exos was determined by the bicinchoninic acid (BCA) method (Beyotime, Shanghai, China). Finally, Exos were stored at -80°C for later use.

*Drug entrapment*

A total of 40 μL of Exos and 60 μg of FU were mixed evenly using buffer to establish a system (200 μL). Following electroporation at room temperature, 1,000 V and 20 ms, the mixture was stored at 4°C [22], and blank-DC-Exos group (Control group) and FU-DC-Exos group (Experiment group) were set.

*Identification of Exos*

The morphology of Exos was observed using biological TEM. 20 μL of Exos harvested by the ultrahigh-speed centrifugation, PEG precipitation and kit methods were taken, added dropwise to a copper mesh, and blotted up using filter paper 1 min later. Then, a drop of 1% uranyl acetate was added and absorbed using filter paper 1 min later. Subsequently, the resulting Exos were baked dry using an incandescent lamp, and observed and photographed under a TEM.

The particle size distribution and concentration of Exos were determined using NTA. The reserved DC-Exos and FU-DC-Exos solution was separately diluted at 1:7,500 to 10 mL, and the instrument parameters were set for loading and calculating the concentrations of DC-Exos and FU-DC-Exos in cell supernatant.

The expression of Exos-specific proteins was detected via Western blotting as follows: Total proteins were extracted from CT26 cells, DC-Exos and FU-DC-Exos, and after quantification, the concentration of the proteins was adjusted. Finally, the expressions of Exos marker proteins CD9, TSG101 and Alix (rabbit anti-human monoclonal antibodies 1:1,000) were measured using Western blotting.

*Analysis of uptake of Exos using laser confocal microscope*

Exos were labeled using 3,3'-dioctadecyloxacarbocyanine perchlorate (DiO), a green fluorescence probe for cell membranes: DC-Exos were re-suspended in 1 mL of freshly prepared DiO stain with a final concentration of 10 μM. Then. the labeled DC-Exos were centrifuged at 120,000 g for 2 h to remove the remaining stain, and the precipitates were re-suspended in 20 μL of PBS. Subsequently, the above-mentioned DiO-labeled DC-Exos were incubated at 20 μg/mL in 6-well plates with cell slides, and fixed using 4% PFA. After that, each well was added with 500 μL of 4',6-diamidino-2-phenylindole (DAPI) to stain cell nuclei for 10 min, and rinsed using PBS for 5 min×3 times, and 100 μL of F-actin added into each well to stain cytoskeletons and incubate with the DC-Exos in the dark for 10 min. With the F-actin aspirated, the resulting DC-Exos were rinsed using PBS for 5 min×3 times, and the slides were blocked. Finally, the images of all the prepared cell slides were acquired using a confocal microscope and analyzed with Image J software (Rawak Software, Inc., Hamburg, Germany).

*Detection of influence of FU on CT26 cell proliferation ability through methyl thiazolyl tetrazolium (MTT) assay*

CT26 cells in the logarithmic growth phase were taken, digested using 0.25% trypsin solution, prepared into single-cell suspension, and inoculated into 96-well culture plates at $5.2\times10^3$ cells/well, and they were treated with blank DC-Exos (40 μg/mL) (DC-Exos group), FU solution (40 μg/mL) (FU group), FU-DC-Exos (FU concentration: 40 μg/mL) (FU-DC-Exos group) or nothing (Control group), with 6 replicated wells set in each group. Then, the culture plates were placed in the incubator with 5% $CO_2$ at 37°C and incubated for 24, 48, and 72 h. After each well was added with 20 μL of MTT solution and placed in the incubator for 4 h, the supernatant was discarded. Finally, each well was added with 150 μL of DMSO solution, and the optical density was measured using a microplate reader at a wavelength of 490 nm.

*Evaluation of CT26 cell apoptosis via DAPI staining*

CT26 cells were seeded into a 6-well culture plates at $5\times10^5$ cells/well, and after adherence, they were treated with blank DC-Exos (40 μg/mL) (DC-Exos group), FU solution (40 μg/mL) (FU group), FU-DC-Exos (FU concentration: 40 μg/mL) (FU-DC-Exos group) or nothing (Control group), with 3 replicated wells set in each group.

*Measurement of cell migration ability via wound healing assay*

The culture plate into which no cells were inoculated was marked on the back, and after digestion, cells were seeded into the 6-well plates and treated with blank DC-Exos (40 μg/mL) (DC-Exos group), FU solution (40 μg/mL) (FU group), FU-DC-Exos (FU concentration: 40 μg/mL) (FU-DC-Exos group) or PBS solution (Control group) for 24 h, with 3 replicated wells set in each group. When cells were paved onto the whole bottom of the plate, cell scratches were made using a 1 mL pipette tip perpendicular to the plate, and the width of each scratch should be as consistent as possible. Subsequently, with the culture medium discarded, the plate was rinsed using PBS for 3 times to wash away cell debris caused by scratching, and the cells were photographed at T0, cultured for another 24 h and photographed again to observe the migration at T24. Finally, the distance of cell scratches was calculated using ImageJ software, and the migration rate of cells was detected based on cell migration rate (%) = (width at T0 - width at T24)/ width at T0 ×100%. The experiment was repeated for three times.

*Establishment of tumor-bearing BALB/c mouse model of colon cancer*

The CT26 cell tumor-bearing mouse model was established, and FU was injected into tail veins to research the anti-tumor effect *in vivo*. Healthy BALB/c mice aged 5-6 weeks old and weighing about 20 g were subcutane-

ously inoculated with CT26 cells at $1\times10^6$ cells/mouse through the right anterior armpit, and when the volume of tumors reached 50-100 $mm^3$, the tumor-bearing mice were randomly divided into 4 groups, namely Control group (n=10), DC-Exos group (n=10), FU group (n=10) and FU-DC-Exos group (n=10). FU was injected into tail veins at a dose of 30 mg/kg every other day for 7 times in total. The mice were weighed every other day, and the changes in weight were recorded. Meanwhile, the longest diameter (a) and the shortest diameter (b) of tumors were measured using a vernier caliper, and the tumor volume (V) was calculated based on the formula $V=ab^2/2$. Following drug administration for 2 weeks, the mice were sacrificed through cervical dislocation at 24 h after the last drug administration, and the tumor tissues were stripped and weighed.

*Detection of apoptosis in tumor tissues via terminal deoxynucleotidyl transferase-mediated dUTP nick end labeling (TUNEL)*

Paraffin-embedded mouse tumor tissue sections were routinely de-paraffinized and dehydrated with gradient ethanol, incubated with 20 mg/L protease K dissolved in Tris/HCl at room temperature for 15 min, and washed using PBS for 5 min×2 times. Then, the sections were added with 50 μL of TUNEL reaction mixture, incubated at 37°C for 60 min and rinsed with PBS for 5 min×3 times. The resulting sections were dehydrated in gradient ethanol, transparentized using xylene, sealed in neutral resin and observed under a light microscope. Three pieces of sections were taken from each mouse in all groups, and five fields were selected in each section under a light microscope (×200). Finally, the number of apoptotic cells in each field was counted using Image-Pro Plus software (Version X; Media Cybernetics, Silver Springs, MD, USA), with the mean as the number of positive cells at the tumor site of the mouse.

*Hematoxylin-eosin (H&E) staining*

Different FU was injected into the CT26 cell tumor-bearing mouse models through tail veins to preliminarily study the toxicity of FU. CT26 cell tumor-bearing mice were randomly assigned into four groups and injected with PBS, DC-Exos, FU-DC-Exos (30 mg/kg FU) and FU-DC-Exos (60 mg/kg FU), respectively, through tail veins once every other day. After drug administration for 7 times, the mice were euthanised, and their vital organs the heart, liver, spleen, lungs and kidneys were taken and prepared into treatment sections.

*Statistics*

All experiments were performed in triplicate at least, and data were processed using SPSS 17.0 software (SPSS IBM, Armonk, NY USA). Measurement data were expressed as mean±standard deviation. Comparison between multiple groups was done using One-way ANOVA test followed by *Post Hoc* Test (Least Significant Difference). The survival curves were plotted using the Kaplan-Meier method and differences were evaluated with log-rank test. $P<0.05$ represented that the differences were statistically significant.

## Results

*Identification results of Exos*

According to the TEM results (Figure 1A,1B), the particle size of Exos obtained through ultrahigh-speed centrifugation was about 100 nm, consistent with 30-150 nm reported in the literature. After staining, it could be seen that Exos had an intact capsule structure in a typical cup shape. Additionally, drug-loaded Exos exhibited no obvious change in morphology and a distinct saucer-like double-layer membrane structure, which were distributed alone or congregated in groups, with clearer background and fewer contaminants (Figure 1B).

The particle size and number of DC-Exos and FU-DC-Exos were measured using NTA, and according to the results (Figure 1C), the mean density of particles was mostly 110 nm, suggesting an intensive particle size distribution of samples. With 160 nm as the boundary between Exos and other vesicles, the calculation results revealed that the particle number of Exos extracted represented over 89% of the total. After precipitates of Exos were diluted with PBS 7,000 folds, the concentration was measured as $2\text{-}6\times10^7$/mL using TEM. The particle size of FU-DC-Exos was slightly increased (Figure 1D), which is consistent with the results in the literature reports, partly because FU is embedded into the phospholipid bilayer sites of Exos and hydrophobic interactions causes surface absorption [23,24].

The Exos-specific marker proteins, namely membrane CD9 and internal proteins, Alix and TSG101, were detected via Western blotting (Figure 1E). In this experiment, it was found that the proteins extracted from the precipitates of Exos through ultrahigh-speed centrifugation contained positively expressed CD9, Alix and TSG101, and their expression levels were higher than those in CT26 cells, indicating that Exos were obtained by the ultrahigh-speed centrifugation method. Moreover, drug loading had no evident influence on the expression of Exos-specific proteins.

*Uptake of Exos*

As shown in Figure 2, DAPI-stained cell nuclei are blue, phalloidin-labeled cytoskeletons are red, and DiO-labeled Exos are green. The green fluorescence in the merge images was clear and visible and distributed in the cytoplasm, whereas red fluorescence was also seen in CT26 cells after the phalloidin-stained cytoskeletal protein. F-actin was stained with Rhodamine 123, suggesting that DiO-labeled Exos can be taken in by CT26 cells.

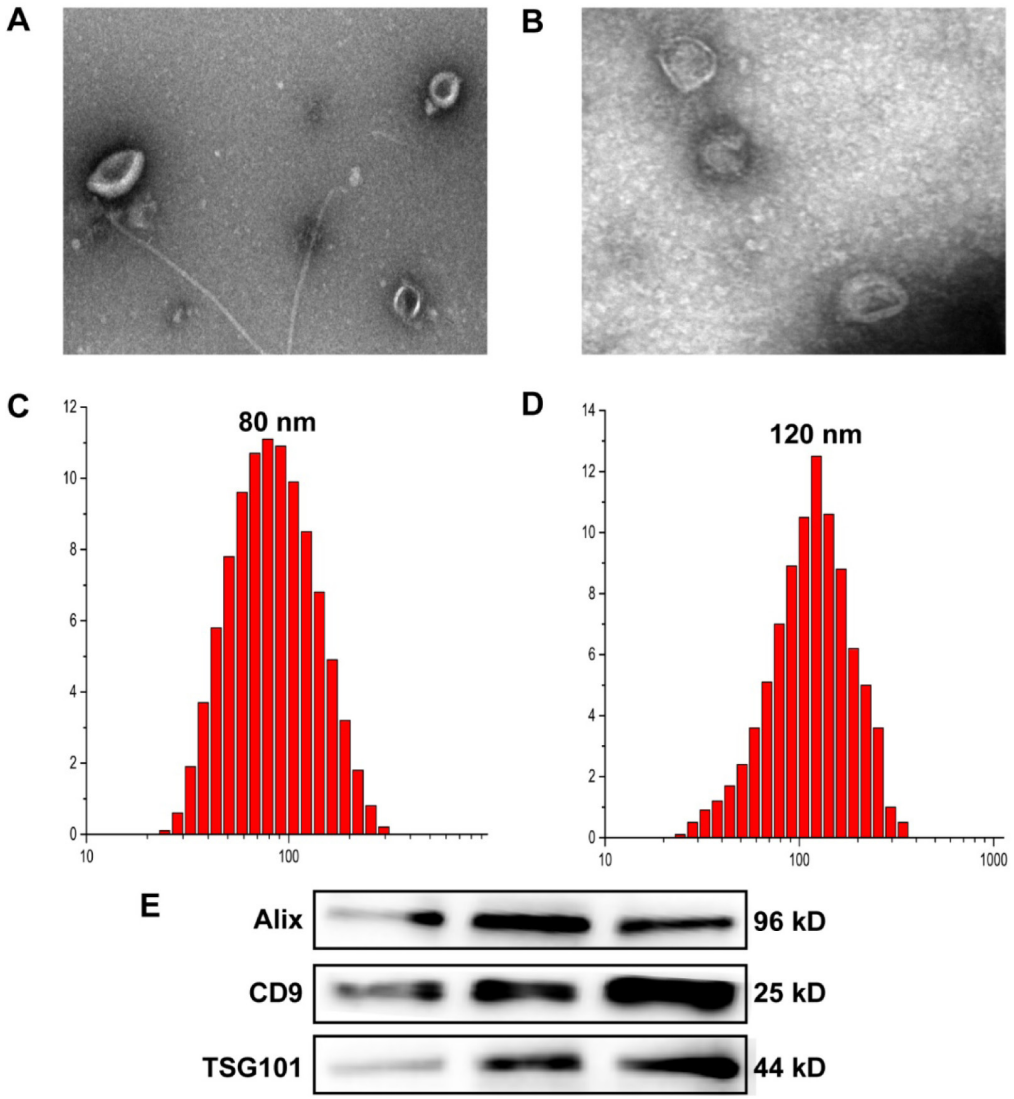


**Figure 1.** Identification of Exos. **A, B:** Morphology of Exos observed by TEM. **C, D:** Particle size of NK-Exos analyzed using NTA. **E:** Expressions of Exos specific proteins analyzed using Western blotting and showing that the proteins extracted from the precipitates of Exos through ultrahigh-speed centrifugation contained positively expressed CD9, Alix and TSG101, and their expression levels were higher than those in CT26 cells.

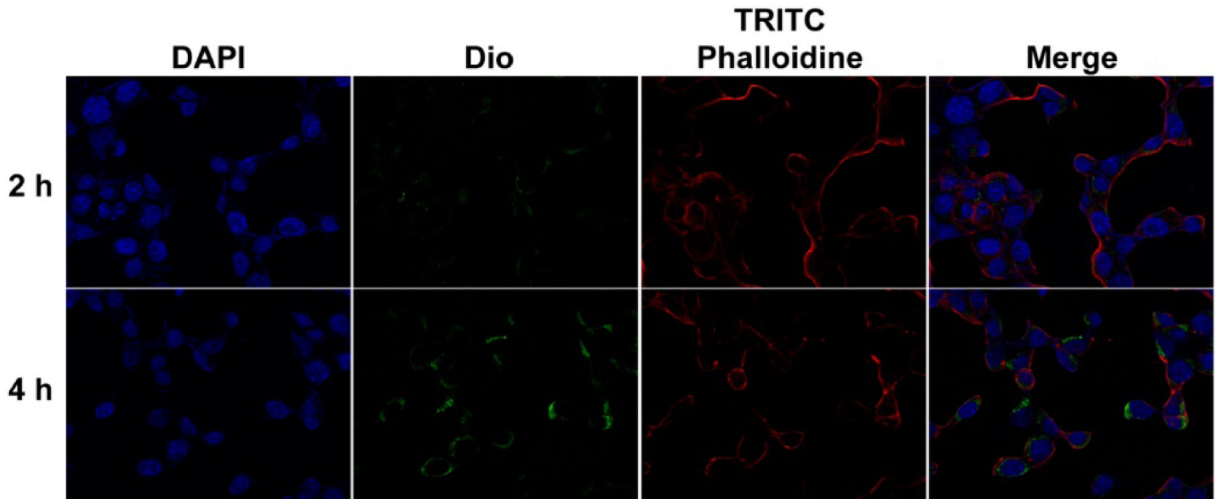


**Figure 2.** Uptake of Exos. Uptake of Exos in CT26 cells is observed using the laser confocal microscope. DAPI-stained nuclei, Dio-stained Exos, and Rhodamine-labeled phalloidine-stained cytoskeleton.

*FU-DC-Exos promoted CT26 cell apoptosis*

The MTT assay results revealed that the viability of CT26 cells in FU and DC-Exos groups was weakened at 24, 48 and 72 h compared with that in the Control group (*p<0.05, *p<0.05, *p<0.05) (Figure 3A). The viability of CT26 cells at 24, 48 and 72 h in FU-DC-Exos group was obviously weaker than that in FU group ($^{\#}$p<0.01, $^{\#}$p<0.01, $^{\#}$p<0.01).

Likewise, the DAPI staining results (Figure 3B) manifested that the inhibitory effect of the preparation FU-DC-Exos on CT26 cell proliferation was more significant than that of dissociative FU at the same concentration, whereas the inhibitory effect of DC-Exos alone was not markedly different from that of DCs. The cells in the Control group exhibited diffusely and evenly distributed blue fluorescence in cell nuclei, while those in the FU group showed a small spot of blue glow in most cell nuclei or blue glow in few cell nuclei, implying that the cells had significant apoptosis findings. Compared with that in the FU group, the trend of inducing cell apoptosis was more obvious in the FU-DC-Exos group.

*Influence of FU-DC-Exos on CT26 cell migration ability*

According to the results of cell wound heal-

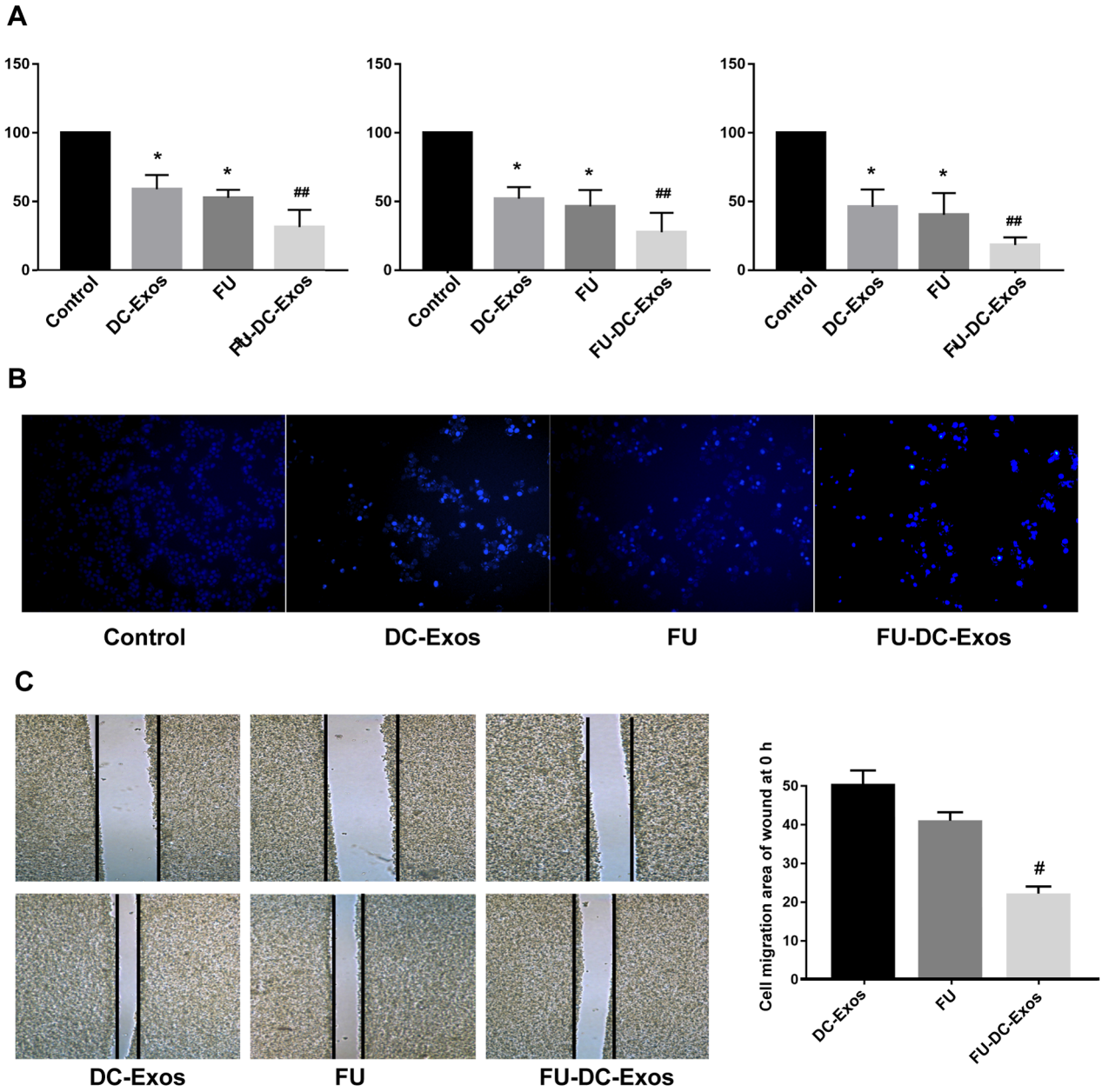


**Figure 3.** CT26 cell apoptosis assay. **A:** Survival rate of CT26 cells at 24 h, 48 h and 72 h detected using MTT assay. **B:** Apoptosis of CT26 cells detected using DAPI staining. **C:** FU-DC-Exos inhibits migration of CT26 cells (*p<0.05 compared with the control group, $^{\#\#}$p<0.01 compared with the control group, $^{\#}$p<0.05 compared with FU group).

ing assay (Figure 3C), the migration of CT26 cells was markedly repressed in both DC-Exos and FU groups, while the migration rate of CT26 cells in FU-DC-Exos group was lower than that in the FU group ($^{\#}p<0.01$).

*In vivo pharmacodynamic experiment results of FU-DC-Exos*

Figure 4 presents the efficacy of different FU systems and PBS in the CT26 tumor-bearing mice after tail vein administration for 14 days. Based on the experimental results, the volume of tumors was notably increased in Control group (Figure 4A,4B), whereas the growth of tumors was suppressed by DC-Exos, FU and FU-DC-Exos, among which FU-DC-Exos had the strongest inhibitory ability, followed by FU and DC-Exos. At the end of treatment, tumors were taken from the mice in each group and weighed, and the tumor weight in all groups was 1.12±0.30 g, 0.71±0.05 g, 0.51±0.01 g, and 0.40±0.03 g, respectively (Figure 4C, 4D).

*Toxicity test results of vital organs*

Toxic side effects are also important indicators for evaluating novel carriers, and the safety of the FU delivery system can be assessed through analyzing animal weight. According to the changes in mouse weight during the whole treatment process, the mice administered with FU had distinctly decreased weight at the end of treatment, while those

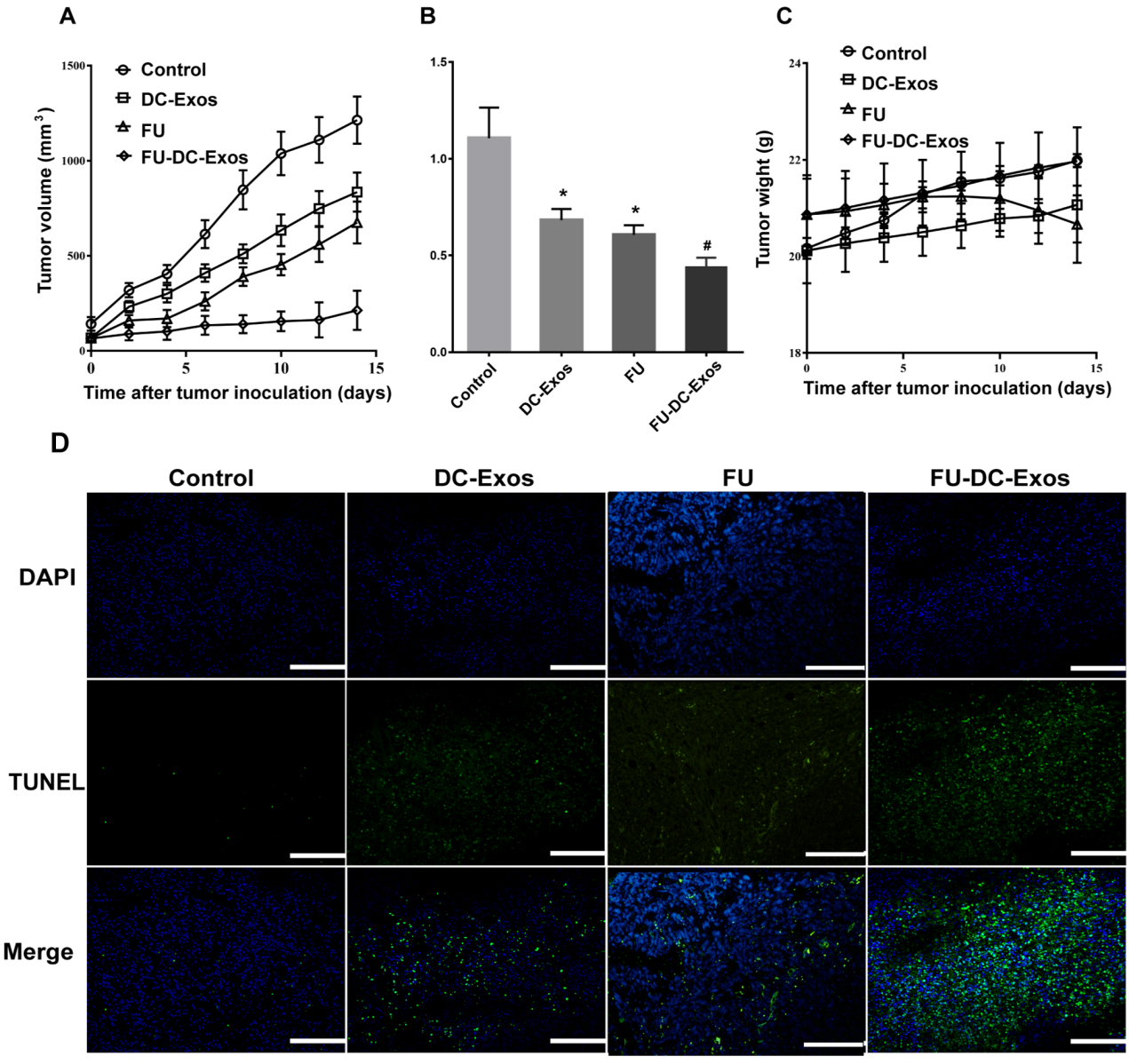


**Figure 4.** *In vivo* antitumor efficacy in CT26-tumor bearing mice model. **A:** tumor growth curves; **B:** tumor weight; **C:** body weight changes (Mean ± SD, n =10, *p<0.05 compared with the control group, #p<0.01 compared with FU group); **D:** the tumor cells apoptosis were detected by TUNEL assay in each group.

in the other groups had steadily increased weight in the whole process. At the same time, the mice in FU-DC-Exos group were healthy and energetic in the whole treatment period. Additionally, the H&E (Figure 5) staining results further corroborated the safety of FU-DC-Exos system: after the mice were given a 2-fold dose of FU (40 mg/kg) for 7 times, the organs of mice were collected, and no notable injuries were found.

The nano drug delivery system FU-DC-Exos has a favorable anti-tumor effect and extremely few systemic toxic side effects, thereby serving as a good supplement for the treatment with FU. Moreover, FU's treatment effect is to affect the mitosis of the nuclei, and as the endogenous substances, DC-Exos can deliver FU into tumor cells more effectively, thus increasing the cellular internalization of FU and enhancing its therapeutic effect.

## Discussion

As a representative of a class of crucial anti-tumor drugs, FU plays an important role in treating various malignancies such as colon cancer [25]. Since FU itself is greatly toxic, after drug administration, the patients are prone to severe adverse reactions, such as myelosuppression, and damage to gastrointestinal and nervous system, which seriously hinders the extensive clinical application of FU. With the rapid development of drug delivery systems, nanotechnology holds promise for application because it can target and control drug release, and various types of nanocarriers are able to remarkably improve the therapeutic effect of drugs [26].

In addition, Exos, as endogenous nanoscale membrane vesicles, have received attention from more and more researchers for the advantages in drug delivery systems. A study found that Exos-biomimetic nanoparticles, can effectively deliver the hydrophilic drug doxorubicin to tumor sites and kill the tumors [27]. Another study compared Exos with ferritin nanocage in delivering the membrane protein therapeutic agent, and discovered that the therapeutic index of Exos in mediating the inhibition on tumor growth by CD47 blockage is higher than that of ferritin-SIRPα, indicating the significance of the unique characteristics of Exos, especially the phospholipid bilayer membrane scaffold, in improving protein delivery [17]. Exos can transport small interfering (si) RNAs to treat Hun-

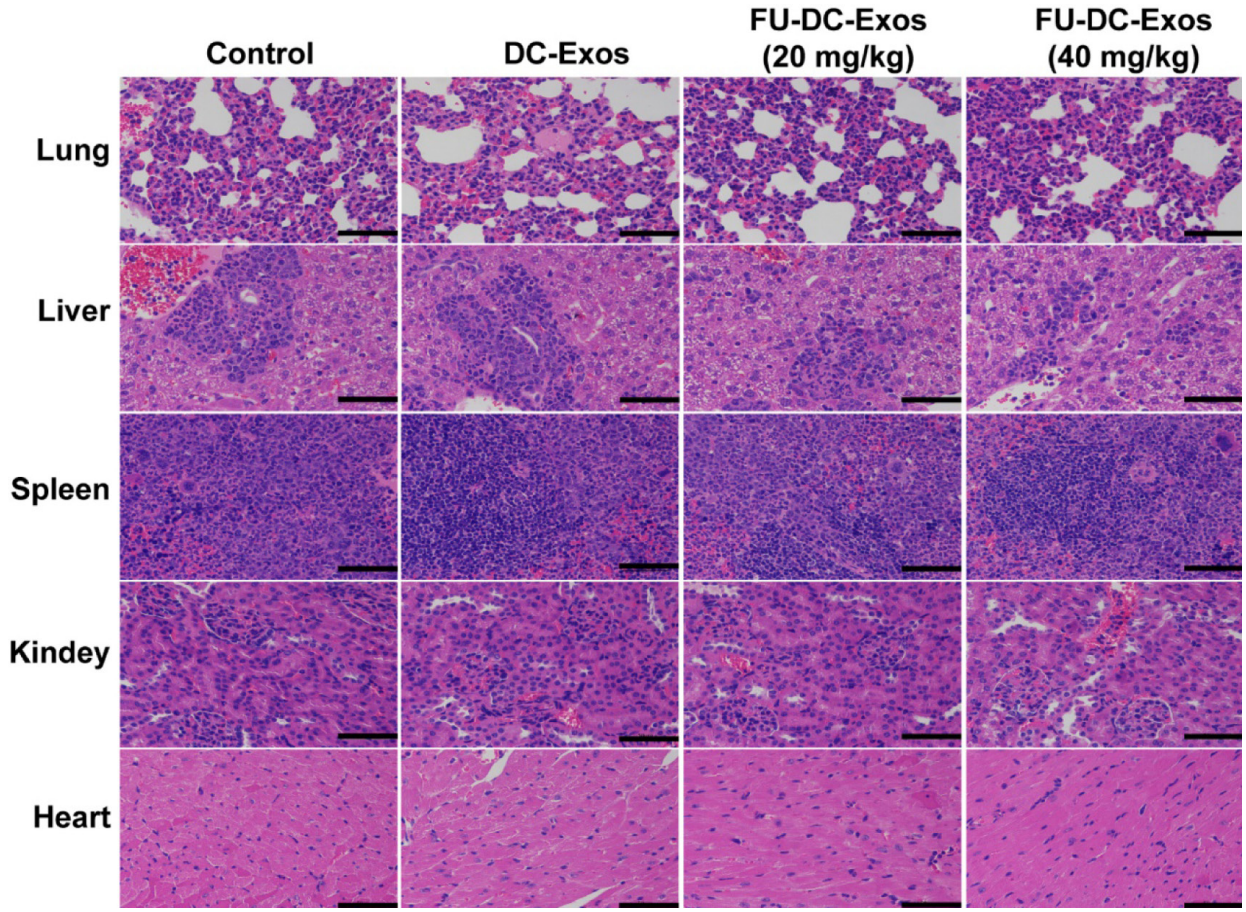


**Figure 5.** Safety evaluation: H&E staining of the major organs harvested from CT26-tumor bearing mice (magnification ×400).

tington's disease as well. The Exos that can deliver siRNAs to the brain are extensively distributed and efficacious, so they are expected to improve and treat Huntington's disease and other neurological diseases [28]. Exos, as drug and gene carriers, now have become hotspots in researching disease treatment and drug carriers.

In this study, with DC-Exos as the delivery carrier of FU, the DC-Exos-FU delivery system was successfully prepared. First, the particle size of Exos was characterized by means of NTA before and after drug loading, and the results showed that the mean particle size of Exos was increased from 96 nm to 134 nm after drug loading. According to a study, FU is entrapped partly in the phospholipid bilayer of Exos, so the drug-loaded Exos have a slightly larger particle size [29]. To verify the influence of drug loading on the nature of Exos, the surface protein, morphology and potential of drug-loaded Exos were also evaluated in the present study. The Western blotting results manifested that drug loading did not affect the protein abundance of Exos, and the TEM results revealed that the morphology and structure of drug-loaded Exos remained basically unchanged as well. Therefore, drug loading has no obvious effect on the properties of Exos, such as morphology and structure, and drug-loaded Exos still possess all the properties of Exos.

According to the anti-tumor experiment results, compared with FU injection, the FU-DC-Exos delivery system containing an equal dose of FU exhibited a higher inhibition rate in mouse colon cancer CT26 cells. Research has explained such a phenomenon and discovered that the phospholipid bilayer of Exos can directly target fusion cells, thereby increasing the cellular internalization of FU and improving the therapeutic effect [30].

## Conclusions

In this paper, with FU widely applied clinically as a model drug, Exos extracted from DC by the canonical ultrahigh-speed centrifugation were taken as its delivery system, and the FU-DC-Exos system was prepared using electroporation, thereby establishing a chemotherapeutic agent-loaded natural carrier delivery system. Furthermore, the extraction of carriers, and the preparation, characterization and *in vitro* pharmacodynamic activity of the drug delivery system were evaluated to confirm the anti-tumor activity of the drug-loaded system.

## Conflict of interests

The authors declare no conflict of interests.

## References


1. Wicki A, Witzigmann D, Balasubramanian V, Huwyler J. Nanomedicine in cancer therapy: challenges, opportunities, and clinical applications. J Control Release 2015;200:138-57.
2. Liu GY, Lv X, Wu YS et al. Effect of induction chemotherapy with cisplatin, fluorouracil, with or without taxane on locoregionally advanced nasopharyngeal carcinoma: a retrospective, propensity score-matched analysis. Cancer Commun (Lond) 2018;38:21.
3. Tang X, Sun J, Ge T et al. Pegylated liposomes as delivery systems for Gambogenic acid: Characterization and in vitro/in vivo evaluation. Colloids Surf B Biointerfaces 2018;172:26-36.
4. Kang W, Hou X, Wang P et al. Study on the effect of the organic acid structure on the rheological behavior and aggregate transformation of a pH-responsive wormlike micelle system. Soft Matter 2019;15:3160-7.
5. Antunes FE, Marques EF, Miguel MG, Lindman B. Polymer-vesicle association. Adv Colloid Interface Sci 2009;147:18-35.
6. Mangadlao JD, Wang X, McCleese C et al. Prostate-Specific Membrane Antigen Targeted Gold Nanoparticles for Theranostics of Prostate Cancer. Acs Nano 2018;12:3714-25.
7. Jiang XC, Gao JQ. Exosomes as novel bio-carriers for gene and drug delivery. Int J Pharm 2017;521:167-75.
8. Smith JA, Leonardi T, Huang B, Iraci N, Vega B, Pluchino S. Extracellular vesicles and their synthetic analogues in aging and age-associated brain diseases. Biogerontology 2015;16:147-85.
9. Clayton A, Harris CL, Court J, Mason MD, Morgan BP. Antigen-presenting cell exosomes are protected from complement-mediated lysis by expression of CD55 and CD59. Eur J Immunol 2003;33:522-31.
10. Haney MJ, Klyachko NL, Zhao Y et al. Exosomes as drug delivery vehicles for Parkinson's disease therapy. J Control Release 2015;207:18-30.
11. van den Boorn JG, Schlee M, Coch C, Hartmann G. SiRNA delivery with exosome nanoparticles. Nat Biotechnol 2011;29:325-6.
12. Morse MA, Garst J, Osada T et al. A phase I study of dexosome immunotherapy in patients with advanced non-small cell lung cancer. J Transl Med 2005;3:9.
13. Besse B, Charrier M, Lapierre V et al. Dendritic cell-derived exosomes as maintenance immunotherapy after first line chemotherapy in NSCLC. Oncoimmunology 2016;5:e1071008.

14. Dai S, Wei D, Wu Z et al. Phase I clinical trial of autologous ascites-derived exosomes combined with GM-CSF for colorectal cancer. Mol Ther 2008;16:782-90.
15. Viaud S, Ploix S, Lapierre V et al. Updated technology to produce highly immunogenic dendritic cell-derived exosomes of clinical grade: a critical role of interferon-gamma. J Immunother 2011;34:65-75.
16. Kim MS, Haney MJ, Zhao Y et al. Development of exosome-encapsulated paclitaxel to overcome MDR in cancer cells. Nanomedicine-Uk 2016;12:655-64.
17. Cho E, Nam GH, Hong Y et al. Comparison of exosomes and ferritin protein nanocages for the delivery of membrane protein therapeutics. J Control Release 2018;279:326-35.
18. Lu Z, Zuo B, Jing R et al. Dendritic cell-derived exosomes elicit tumor regression in autochthonous hepatocellular carcinoma mouse models. J Hepatol 2017;67:739-48.
19. Munich S, Sobo-Vujanovic A, Buchser WJ, Beer-Stolz D, Vujanovic NL. Dendritic cell exosomes directly kill tumor cells and activate natural killer cells via TNF superfamily ligands. Oncoimmunology 2012;1:1074-83.
20. Kourembanas S. Exosomes: vehicles of intercellular signaling, biomarkers, and vectors of cell therapy. Annu Rev Physiol 2015;77:13-27.
21. Wang P, Wang H, Huang Q et al. Exosomes from M1-Polarized Macrophages Enhance Paclitaxel Antitumor Activity by Activating Macrophages-Mediated Inflammation. Theranostics 2019;9:1714-27.
22. Wlaschek M, Tantcheva-Poor I, Naderi L et al. Solar UV irradiation and dermal photoaging. J Photochem Photobiol B 2001;63:41-51.
23. Liu Z, Jiao Y, Wang Y, Zhou C, Zhang Z. Polysaccharides-based nanoparticles as drug delivery systems. Adv Drug Deliv Rev 2008;60:1650-62.
24. Viaud S, Terme M, Flament C et al. Dendritic cell-derived exosomes promote natural killer cell activation and proliferation: a role for NKG2D ligands and IL-15Ralpha. PLoS One 2009;4:e4942.
25. Herrmann R. Systemic treatment of colorectal cancer. Eur J Cancer 1994;30A:404-9.
26. Lin X, Wu Z, Wu Y, Xuan M, He Q. Self-Propelled Micro-/Nanomotors Based on Controlled Assembled Architectures. Adv Mater 2016;28:1060-72.
27. Yong T, Zhang X, Bie N et al. Tumor exosome-based nanoparticles are efficient drug carriers for chemotherapy. Nat Commun 2019;10:3838.
28. Didiot MC, Hall LM, Coles AH et al. Exosome-mediated Delivery of Hydrophobically Modified siRNA for Huntingtin mRNA Silencing. Mol Ther 2016;24:1836-47.
29. Sobo-Vujanovic A, Munich S, Vujanovic NL. Dendritic-cell exosomes cross-present Toll-like receptor-ligands and activate bystander dendritic cells. Cell Immunol 2014;289:119-27.
30. Cui S, Cheng Z, Qin W, Jiang L. Exosomes as a liquid biopsy for lung cancer. Lung Cancer 2018;116:46-54.